

## Experimental generation of pseudo-bound-entanglement

Hermann Kampermann\* and Dagmar Bruß

*Institut für Theoretische Physik III, Heinrich-Heine-Universität Düsseldorf, D-40225 Düsseldorf, Germany*

Xinhua Peng

*Experimentelle Physik IIIa, Technische Universität Dortmund, D-44221 Dortmund, Germany and Hefei National Laboratory for Physical Sciences at Microscale and Department of Modern Physics, University of Science and Technology of China, Hefei, Anhui 230026, People's Republic of China*

Dieter Suter

*Experimentelle Physik IIIa, Technische Universität Dortmund, D-44221 Dortmund, Germany*

(Received 18 September 2009; published 30 April 2010)

We use nuclear magnetic resonance to experimentally generate a bound-entangled (more precisely: pseudo-bound-entangled) state, i.e., a quantum state which is nondistillable but nevertheless entangled. Our quantum system consists of three qubits. We characterize the produced state via state tomography to show that the created state has a positive partial transposition with respect to any bipartite splitting, and we use a witness operator to prove its pseudoentanglement.

DOI: [10.1103/PhysRevA.81.040304](https://doi.org/10.1103/PhysRevA.81.040304)

PACS number(s): 03.67.Bg, 33.25.+k

Quantum entanglement has been a source of fascination and surprise for more than 70 years [1]. The discovery that entanglement can serve as a resource for information processing has triggered the development of the broad field of quantum-information science [2–5]. Designing and controlling entangled quantum states has thus become a major experimental challenge. Several types of entangled states have already been experimentally generated and detected in the recent years, e.g., bipartite entanglement [6,7], tripartite entanglement [8–10], as well as multipartite entanglement [11–14].

A particularly interesting class of entangled states are “bound-entangled” states [15], which carry quantum correlations of an especially elusive and fragile type. The name “bound entanglement” implies an analogy to bound energy in thermodynamics, which cannot be freed to perform work. Bound entanglement can be described as inherent quantum correlations, without the typical information-processing potential of “free” entanglement. Namely, some correlations of quantum nature are initially established during the generation of a bound-entangled state, but nevertheless it is not possible to extract a maximally entangled state for any number of copies of the state (i.e., entanglement distillation is not possible for bound-entangled states). However, it has been shown that under certain circumstances, bound entanglement can nevertheless be useful to establish a secret key [16]. Bound entanglement is expected to exist in Nature; for example, it has been shown theoretically [17] that thermal states of several spin models carry bound entanglement. Bound-entangled states are always mixed, and because of the small region that they occupy in the space of all states, they are vulnerable to decoherence. Therefore, it is challenging to create and detect them in the laboratory.

Here, we report on an experiment in which pseudo-bound-entanglement is created and observed [18]. We generate a bound-entangled state of a class initially suggested by Acin *et al.* [19] with nuclear magnetic resonance (NMR), and show their nondistillability via state tomography by proving that the partial transpositions are positive. A suitable entanglement witness is implemented to detect the entanglement [20]. As usual in room-temperature liquid-state NMR, we work with states close to the (normalized) identity, i.e., we consider a state of the form

$$\rho = \frac{1-p}{d} \mathbb{1} + p\rho_{\text{BE}}, \quad (1)$$

where  $\rho_{\text{BE}}$  is the bound-entangled density matrix. We therefore call the whole state  $\rho$  pseudo-bound-entangled. This is in analogy with the NMR GHZ state [21]. NMR technology has been widely used to demonstrate quantum-information primitives [22–27], and here it proves again to be a versatile tool.

We consider the family of three-qubit states defined in [19]:

$$\begin{aligned} \rho_{\text{BE}} = N^{-1} & \left( 2|\text{GHZ}\rangle\langle\text{GHZ}| + a_1|001\rangle\langle 001| + a_2|010\rangle\langle 010| \right. \\ & + \frac{1}{a_3}|011\rangle\langle 011| + a_3|100\rangle\langle 100| \\ & \left. + \frac{1}{a_2}|101\rangle\langle 101| + \frac{1}{a_1}|110\rangle\langle 110| \right), \quad (2) \end{aligned}$$

where  $|\text{GHZ}\rangle = \frac{1}{\sqrt{2}}(|000\rangle + |111\rangle)$ , and the normalization is  $N = [2 + \sum_{i=1}^3 (a_i + \frac{1}{a_i})]$ . The free parameters  $a_1, a_2, a_3$  are real positive numbers that obey the condition  $a_1 a_2 a_3 \neq 1$ . This family of states is “almost” diagonal, with the only off-diagonal matrix elements coming from the GHZ contribution; see Fig. 2 for a visual representation. The states have rank 7 and are thus far from being pure. The states in Eq. (2) have a positive partial transposition (PPT) with respect to any

\*kampermann@thphy.uni-duesseldorf.de

bipartite splitting, but it was shown that they are nevertheless entangled [19]. Therefore, they are bound entangled.

In [20], a family of witness operators which detects the bound-entangled states in Eq. (2) was presented. The family of witnesses has the form

$$W = \overline{W} - \varepsilon \mathbb{1}, \quad (3)$$

with

$$\begin{aligned} \overline{W} = & |\text{GHZ}^-\rangle\langle\text{GHZ}^-| + \frac{1}{1+a_1^2}(|001\rangle\langle 001| + a_1^2|110\rangle\langle 110|) \\ & + \frac{1}{1+a_2^2}(|010\rangle\langle 010| + a_2^2|101\rangle\langle 101|) \\ & + \frac{1}{1+a_3^2}(|100\rangle\langle 100| + a_3^2|011\rangle\langle 011|) \\ & - \sum_{i=1}^3 \frac{a_i}{1+a_i^2}(|000\rangle\langle 111| + |111\rangle\langle 000|). \end{aligned} \quad (4)$$

where  $|\text{GHZ}^-\rangle = \frac{1}{\sqrt{2}}(|000\rangle - |111\rangle)$ . Note that we are not using any specific normalization of the witness. We choose the set of free parameters for the state and witness in such a way that the witness detects entanglement with the highest fraction of white noise. The optimal parameters calculated via convex optimization are  $a_1 = a_2 = a_3 = a = 0.3460$  and  $\varepsilon = 0.1069$  [20].

A perfect experimental realization of the bound-entangled state  $\rho_{\text{BE}}$  would lead to the expectation value  $\text{tr}(W\rho_{\text{BE}}) = -\varepsilon$ . This is obvious by construction, as  $\overline{W}$  is decomposable (i.e., it can be written as the sum of a positive operator and the partial transposition of another positive operator), and therefore its expectation value for a PPT bound-entangled state cannot be smaller than zero. In fact,  $\text{tr}(\overline{W}\rho_{\text{BE}}) = 0$ . The expectation value for the identity part gives  $-\varepsilon$ . The smallest possible expectation value of the witness  $W$  is achieved by the GHZ state  $|\text{GHZ}\rangle = \frac{1}{\sqrt{2}}(|000\rangle + |111\rangle)$ , because this is the eigenvector corresponding to the negative eigenvalue of the witness ( $\lambda = -\frac{3a}{1+a^2} - \varepsilon \approx -1.03$ ). Therefore, the minimal expectation value for a bound-entangled state is only about 1/10 of the minimal expectation value for a free-entangled state. This is one of the reasons why the detection of bound entanglement is experimentally much more challenging than the detection of free entanglement.

In current liquid NMR experiments, a huge ensemble of about  $\sim 10^{19}$  copies of the quantum processors are used. The ensemble in thermal equilibrium follows the Boltzmann distribution dominated by the spin interaction with the external magnetic field. The equilibrium density operator is well approximated by

$$\rho_{\text{eq}} = \frac{1}{d} \left( \mathbb{1} + \sum_i \kappa_i I_{zi} \right), \quad (5)$$

where  $\kappa_i$  is a spin and system-specific constant given by  $\kappa_i = \frac{\hbar B_0 \gamma_i}{kT}$  with  $\gamma_i$  being the gyromagnetic ratio,  $B_0$  the magnetic field strength,  $k$  the Boltzmann constant, and  $T$  the temperature of the system.  $I_{zi}$  denotes the  $z$  component of the angular momentum operator of the  $i$ th nuclear spin, and  $d$  is the dimension of the total system. In usual liquid NMR

experiments with a magnetic field of  $B_0 \sim 12$  T and protons at ambient temperatures ( $T = 290$  K), we have  $\kappa_{\text{H}} \approx 8.4 \times 10^{-5}$ .

The state of interest in our case is given by Eq. (1), where we want to generate a specific pseudo-bound-entangled state  $\rho$ , i.e., the deviation from the normalized identity, with the probability  $p$  available in our system. Our three-qubit system can reach under the above conditions a fraction of  $p$  for the bound-entangled state on the order of  $\kappa$ . To characterize the properties of  $\rho_{\text{BE}}$  we will do state tomography to reconstruct the experimentally generated state  $\rho_{\text{exp}}$ . Then we will prove entanglement of the part  $\rho_{\text{exp, BE}}$ . For this purpose, we adopt the usual witness formalism to the pseudostate case, i.e., we shift the witness in Eq. (3) by the contribution which comes from the identity; namely, we introduce the ‘‘pseudowitness’’

$$W_{\text{NMR}} = \frac{W - \frac{(1-p)}{d} \mathbb{1}}{p}, \quad (6)$$

such that  $\text{tr}(W_{\text{NMR}}\rho) = \text{tr}(W\rho_{\text{BE}})$ .

We use the heteronuclear three-qubit system ethyl 2-fluoroacetoacetate [28], consisting of a hydrogen, a carbon, and a fluorine spin (see Fig. 1) with gyromagnetic ratios of  $\gamma_{\text{H}} \approx 26.75 \times 10^7$ ,  $\gamma_{\text{C}} \approx 6.73 \times 10^7$ , and  $\gamma_{\text{F}} \approx 25.18 \times 10^7 \text{ T}^{-1} \text{ s}^{-1}$ .

Using such a heteronuclear system has several advantages: first we can apply fast local (spin-specific) unitary operations because of the large Zeeman energy difference between the spins, and second we can focus on the zero-order coupling Hamiltonian in the rotating frame representation,  $H = J_{12}I_{z1}I_{z2} + J_{13}I_{z1}I_{z3} + J_{23}I_{z2}I_{z3}$ . Here,  $J_{12} = 161.3$ ,  $J_{13} = -190.2$ , and  $J_{23} = 47.0$  Hz are the  $J$ -coupling constants between the spins. Couplings with other spins are  $\leq 1$  Hz and can be neglected.

We developed the following experimental strategy:

(i) Generate a suitable basis state population, (ii) Apply unitary transformations (quantum gates) to the diagonal state to generate  $\rho_{\text{BE}}$ , and (iii) Characterize the generated state by state tomography and witnesses.

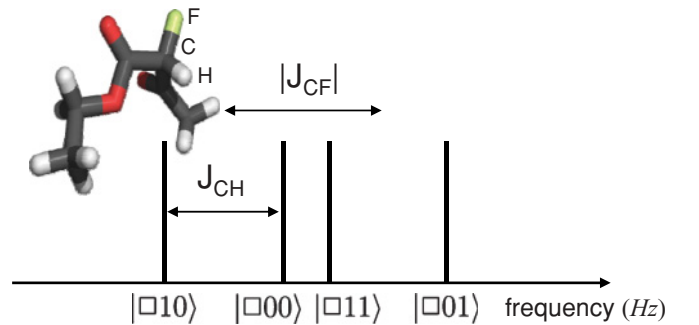


FIG. 1. (Color online) Schematic carbon NMR spectrum of the CHF group of ethyl 2-fluoroacetoacetate and the stick representation of the molecule. The  $J$  couplings between the spins as well as the H,F spin states in the computational basis are presented. We use the spin-state representation of the form  $|C, H, F\rangle$ , i.e., C, H, and F correspond to the first, second, and third qubit, respectively. With the boxes, we denote that the transition  $0 \leftrightarrow 1$  of this spin is observed. The order of the numbering of the spin states in the spectrum is due to the signs of the  $J$ -coupling constants.

In the first part of the experiment, we generate a specific diagonal state, i.e.,

$$\rho_d = \frac{\mathbb{1}}{8} + \frac{p}{8}(d_a I_{z1} + d_b I_{z2} + d_b I_{z3} + d_c I_{z1} I_{z2} + d_c I_{z1} I_{z3} + d_d I_{z2} I_{z3} + d_e I_{z1} I_{z2} I_{z3}), \quad (7)$$

with the coefficients  $d_a = \frac{2[(a-2)a-1]}{a(3a+2)+3} \approx -0.78$ ,  $d_b = -\frac{2(a+1)^2}{a(3a+2)+3} \approx -0.21$ ,  $d_c = 2d_a$ ,  $d_d = 2d_b$ , and  $d_e = \frac{48}{a(3a+2)+3} - 8 \approx 3.85$ . We scaled the traceless spin operators in such a way that the scaling factor  $p$  of this deviation density operator corresponds to the probability of our pseudo-bound-entangled state of Eq. (1).

Five experiments are performed to generate different basis state populations. The five diagonal states have the form

$$\begin{aligned} \rho_1 &= \frac{\mathbb{1}}{8} + \frac{\kappa_H}{8}(3.77I_{z1}I_{z2}I_{z3}), \\ \rho_2 &= \frac{\mathbb{1}}{8} + \frac{\kappa_H}{8}(-2I_{z1}I_{z2}), \\ \rho_3 &= \frac{\mathbb{1}}{8} + \frac{\kappa_H}{8}(-1.88I_{z1}I_{z3}), \\ \rho_4 &= \frac{\mathbb{1}}{8} + \frac{\kappa_H}{8}(-2I_{z2}I_{z3}), \\ \rho_5 &= \frac{\mathbb{1}}{8} + \frac{\kappa_H}{8}(-I_{z1} - 0.27I_{z2} - 0.27I_{z3}). \end{aligned} \quad (8)$$

The manipulation of the equilibrium states to generate each of these states is done by standard hard spin selective pulses,  $J$ -coupling evolution [3], and at the end  $z$  gradients to destroy the unwanted ( $x$ ,  $y$ ) magnetization terms, i.e., we apply spatial averaging [29].

The states of these experiments are added with appropriate probabilities to achieve our diagonal density operator  $\rho_d$  in Eq. (7) (temporal averaging [30,31]), i.e.,

$$\begin{aligned} \rho_d &= \sum_i q_i \rho_i \quad \text{with} \quad \sum_i q_i = 1, \\ q_1 &\approx 0.36, \quad q_2 = q_5 \approx 0.27, \quad q_3 \approx 0.29, \quad q_4 \approx 0.08. \end{aligned} \quad (9)$$

It follows  $p \approx \frac{\kappa_H}{3.61}$ .

For implementing step (ii), we developed a sequence of high-fidelity quantum gates which are applied to the initial state of Eq. (9). In detail, we first apply an effectively line selective  $-\frac{\pi}{2}$  rotation around the  $y$  axis in the space  $|000\rangle$ ,  $|100\rangle$  without affecting the remaining basis states. In the following set of hard rf pulses and  $J$ -coupling evolutions, two gates similar to controlled-NOT gates (with qubit 1 as control, qubit 2 as target, and qubit 3 as target) are applied [21]. The total unitary transformation of these quantum gates is

$$\begin{aligned} U &= \frac{1}{\sqrt{2}}(|000\rangle\langle 000| + |000\rangle\langle 100| - |111\rangle\langle 000| \\ &+ |111\rangle\langle 100|) + i|001\rangle\langle 001| - i|010\rangle\langle 010| \\ &+ |011\rangle\langle 011| + |100\rangle\langle 111| + i|101\rangle\langle 110| - i|110\rangle\langle 101|. \end{aligned} \quad (10)$$

The generated state is characterized by state tomography in the usual NMR setting [30], i.e., before detection, the spin-selective rotations  $Y_1 E_2 E_3$ ,  $E_1 E_2 Y_3$ ,  $E_1 E_2 X_3$ ,  $Y_1 Y_2 E_3$ ,  $E_1 X_2 X_3$ ,  $Y_1 Y_2 Y_3$ , and  $X_1 X_2 X_3$  are performed. Here  $X_i$  ( $Y_i$ )

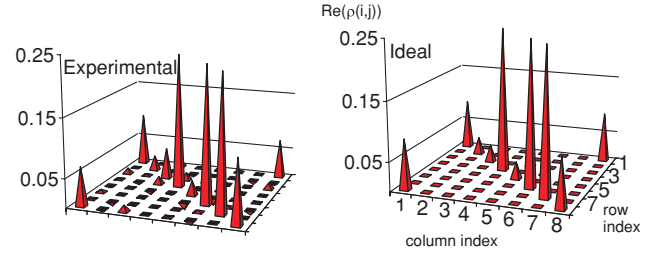


FIG. 2. (Color online) Experimental and ideal real matrix elements of  $\rho_{BE}$ . All imaginary elements of the experimental state are small ( $<0.019$ ).

denotes a  $\pi/2$  rotation of the  $i$ th spin about the  $x$  ( $y$ ) axis and  $E_i$  is the identity operation. In the experiments, only the carbon spin (see Fig. 1) is detected. To get the information of the H (F) spins, an appropriate swap gate to the carbon and H (F) spin is performed before detection. The experimental data gained by this procedure leads to an overdetermined set of linear equations for reconstructing the density matrix. We reconstruct the density operator from the experimental data by a least-squares fit [32].

The experimentally generated state is shown in Fig. 2. The excellent agreement between ideal and generated state reflects the high controllability as well as low decoherence of our NMR system. The main deviations are due to pulse imperfections and partial relaxation during the experiment.<sup>1</sup> Still, partial relaxation has only a small effect, due to  $T_2^* \approx 1$  s and  $T_1 \approx 3$  s in comparison to the total experiment time of roughly 50 ms.

The fraction  $p$  of the pseudo-bound-entangled state in  $\rho_{\text{exp}} = \frac{(1-p)}{8}\mathbb{1} + p\rho_{BE}$  is in our case about  $p \approx 10^{-5}$ .

How close this state is to the ideal one can be expressed in terms of the overlap or the distance between the real and ideal states. We find a high Uhlmann fidelity [33] for the pseudo-bound-entangled state, namely,

$$F_u = \text{tr}\left(\sqrt{\sqrt{\rho_{BE,\text{theo}}}\rho_{BE,\text{exp}}\sqrt{\rho_{BE,\text{theo}}}}\right) = 0.98, \quad (11)$$

and a small trace distance [34],  $d_t = \text{tr}(\sqrt{X^\dagger X})/2 = 0.09$ , with  $X = \rho_{BE,\text{theo}} - \rho_{BE,\text{exp}}$ . The standard deviation of the density operator elements are obtained from the least-squares method. They are used to calculate the standard deviation of the witness expectation value by error propagation. This deviation accounts for the inconsistencies in the overhead of the experimental data, which are due to imperfections in the tomography procedure. The reconstructed state  $\rho_{BE,\text{exp}}$  has a positive partial transposition with respect to any bipartite splitting. The witness expectation value of the experimental state is

$$\text{tr}(W\rho_{BE,\text{exp}}) = -0.029 \pm 0.010, \quad (12)$$

i.e., the state is bound entangled. Here we calculated the expectation value of the witness operator using the reconstructed state. This is more appropriate than to detect the witness directly [35], because some experimental errors are ‘‘averaged’’ during the least-squares method used in the

<sup>1</sup>In the NMR weak measurement scheme, the usual statistical errors due to limited number of individual measurements play no role.

state tomography procedure. The ideal expectation value would have been  $-0.11$ . Remember that the witness expectation value can vary from  $-1.0$  to  $+1.8$ , i.e., the possible range  $-0.11 \leq \langle W \rangle < 0$  for bound entanglement is rather small; thus, already small deviations from the ideal situation can have large effects. The same remark holds for the eigenvalues of the partial transposition.

In conclusion, we have generated and detected pseudo-bound-entanglement with a NMR experiment. A sequence of implementable quantum operations for the generation of pseudo-bound-entanglement was developed. We reached a high fidelity,  $F = 0.98$ , of the created state with respect to the ideal one. The partial transpositions of the state were shown to be positive with respect to any bipartite splitting. The pseudowitness that we used had a negative expectation value, thus proving that the state was indeed pseudoentangled. Thus, we have shown that state-of-the-art control techniques are capable of generating bound entanglement. The framework

of generating this class of states is applicable in general. For example, it can be adopted to the situation of highly polarized spin systems [36,37].

*Note added:* Recently, we learned about related work by Amselem *et al.* [38]. Note, however, that in Table 1 of Ref. [38], five eigenvalues of the partially transposed density matrix are negative (and only compatible with zero via the given error bars), while a necessary condition for the state to be bound entangled is the positivity of all eigenvalues of the partially transposed density matrix.

We thank Otfried Gühne and Matthias Kleinmann for enlightening discussions. We acknowledge financial support from the EU Integrated Projects SCALA and SECOQC, as well as from Deutsche Forschungsgemeinschaft (DFG). X.P. also acknowledges financial support from the Chinese Academy of Science (CAS) and National Natural Science Foundation of China (NNSFC).

- 
- [1] E. Schrödinger, *Naturwissenschaften* **23**, 807 (1935).
  - [2] D. Bruß and G. Leuchs, *Lectures on Quantum Information* (Wiley-VCH, New York, 2007).
  - [3] J. Stolze and D. Suter, *Quantum Computing: A Short Course from Theory to Experiment* (Wiley-VCH, New York, 2004).
  - [4] R. Horodecki, P. Horodecki, M. Horodecki, and K. Horodecki, *Rev. Mod. Phys.* **81**, 865 (2009).
  - [5] O. Gühne and G. Tóth, *Phys. Rep.* **474**, 1 (2009).
  - [6] A. Aspect, P. Grangier, and G. Roger, *Phys. Rev. Lett.* **47**, 460 (1981).
  - [7] Q. A. Turchette, C. S. Wood, B. E. King, C. J. Myatt, D. Leibfried, W. M. Itano, C. Monroe, and D. J. Wineland, *Phys. Rev. Lett.* **81**, 3631 (1998).
  - [8] D. Bouwmeester, J. W. Pan, M. Daniell, H. Weinfurter, and A. Zeilinger, *Phys. Rev. Lett.* **82**, 1345 (1999).
  - [9] D. Leibfried, M. Barrett, T. Schaetz, J. Britton, J. Chiaverini, W. Itano, J. Jost, C. Langer, and D. Wineland, *Science* **304**, 1476 (2004).
  - [10] C. Roos, M. Riebe, H. Häffner, W. Hänsel, J. Benhelm, G. Lancaster, C. Becher, F. Schmidt-Kaler, and R. Blatt, *Science* **304**, 1478 (2004).
  - [11] M. Bourennane, M. Eibl, C. Kurtsiefer, S. Gaertner, H. Weinfurter, O. Gühne, P. Hyllus, D. Bruß, M. Lewenstein, and A. Sanpera, *Phys. Rev. Lett.* **92**, 087902 (2004).
  - [12] C. Lu, X. Zhou, O. Gühne, W. Gao, J. Zhang, Z. Yuan, A. Goebel, T. Yang, and J. Pan, *Nature Phys.* **3**, 91 (2007).
  - [13] H. Häffner, W. Hänsel, C. Roos, J. Benhelm, D. Chek-al-kar, M. Chwalla, T. Körber, U. Rapol, M. Riebe, P. Schmidt, C. Becher, O. Gühne, W. Dür, and R. Blatt, *Nature* **438**, 643 (2005).
  - [14] D. Leibfried, E. Knill, S. Seidelin, J. Britton, R. Blakestad, J. Chiaverini, D. Hume, W. Itano, J. Jost, C. Langer *et al.*, *Nature* **438**, 639 (2005).
  - [15] M. Horodecki, P. Horodecki, and R. Horodecki, *Phys. Rev. Lett.* **80**, 5239 (1998).
  - [16] K. Horodecki, M. Horodecki, P. Horodecki, and J. Oppenheim, *Phys. Rev. Lett.* **94**, 160502 (2005).
  - [17] G. Tóth, C. Knapp, O. Gühne, and H. J. Briegel, *Phys. Rev. Lett.* **99**, 250405 (2007).
  - [18] H. Kampermann (unpublished).
  - [19] A. Acin, D. Bruß, M. Lewenstein, and A. Sanpera, *Phys. Rev. Lett.* **87**, 040401 (2001).
  - [20] P. Hyllus, C. M. Alves, D. Bruß, and C. Macchiavello, *Phys. Rev. A* **70**, 032316 (2004).
  - [21] R. Laflamme, E. Knill, W. Zurek, P. Catasti, and S. Mariappan, *Philos. Trans. R. Soc. A* **356**, 1941 (1998).
  - [22] J. A. Jones, M. Mosca, and R. H. Hansen, *Nature* **393**, 344 (1998).
  - [23] H. K. Cummins, C. Jones, A. Furze *et al.*, *Phys. Rev. Lett.* **88**, 187901 (2002).
  - [24] D. Suter and T. S. Mahesh, *J. Chem. Phys.* **128**, 052206 (2008).
  - [25] C. A. Ryan, C. Negrevergne, M. Laforest, E. Knill, and R. Laflamme, *Phys. Rev. A* **78**, 012328 (2008).
  - [26] L. M. K. Vandersypen and I. L. Chuang, *Rev. Mod. Phys.* **76**, 1037 (2004).
  - [27] N. Gershenfeld and I. Chuang, *Science* **275**, 350 (1997).
  - [28] J. Zhang, N. Rajendran, X. Peng, and D. Suter, *Phys. Rev. A* **76**, 012317 (2007).
  - [29] D. Cory, M. Price, and T. Havel, *Physica D* **120**, 82 (1998).
  - [30] I. L. Chuang, N. Gershenfeld, M. Kubinec, and D. Leung, *Proc. R. Soc. London A* **454**, 447 (1998).
  - [31] L. M. K. Vandersypen, M. Steffen, G. Breyta, C. S. Yannoni, R. Cleve, and I. L. Chuang, *Phys. Rev. Lett.* **85**, 5452 (2000).
  - [32] G. Long, H. Yan, and Y. Sun, *J. Opt. B: Quantum Semiclass. Opt.* **3**, 376 (2001).
  - [33] A. Uhlmann, *Rep. Math. Phys.* **9**, 273 (1976).
  - [34] M. Nielsen and I. Chuang, *Quantum Computation and Quantum Information* (Cambridge University Press, 2000).
  - [35] O. Gühne, P. Hyllus, D. Bruß, A. Ekert, M. Lewenstein, C. Macchiavello, and A. Sanpera, *Phys. Rev. A* **66**, 062305 (2002).
  - [36] M. S. Anwar, D. Blazina, H. A. Carteret, S. B. Duckett, and J. A. Jones, *Chem. Phys. Lett.* **400**, 94 (2004).
  - [37] T. Maly *et al.*, *J. Chem. Phys.* **128**, 052211 (2008).
  - [38] E. Amselem and M. Bourennane, *Nat. Phys.* **5**, 748 (2009).